Medicinal Chemistry Research (2019) 28:169–181
https://doi.org/10.1007/s00044-018-2274-x

MEDICINAL CHEMISTRY RESEARCH

ORIGINAL RESEARCH

Green synthesis, antileishmanial activity evaluation, and in silico studies of new amino acid-coupled 1,2,4-triazoles

Ahmed M. El-Saghier[1] · Mounier A. Mohamed[1] · Omyma A. Abd-Allah[1] · Asmaa M. Kadry[1] · Tamer M. Ibrahim[2] · Adnan A. Bekhit[3,4]

Received: 23 September 2018 / Accepted: 4 December 2018 / Published online: 22 December 2018

Abstract

Candidates of triazole-containing amino acid derivatives **5a**−**k** were prepared under green chemistry conditions via multicomponent reaction using lemon juice as an acidic catalyst. All compounds were7 characterized by different spectral and elemental analyses. They were evaluated for their in vitro antileishmanial activity against miltefosine and amphotericin B deoxycholate as reference drugs. Compounds **5c**, **5d**, **5e** and **5f** showed superior potencies to miltefosine by 200 folds. These compounds are well tolerated by experimental animals orally up to 250 mg/kg and parenterally up to 100 mg/kg. Reverse docking approach against validated leishmanial targets pinpointed mitogen-activated protein kinase (MAPK) as a possible putative antileishmanial target. In addition, in silico predictions revealed that these compounds exhibited promising drug-likeness and pharmacokinetics profile.

Graphical Abstract

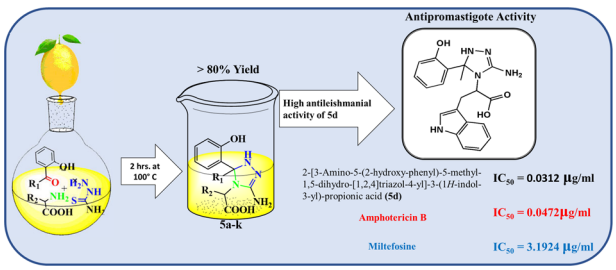

Keywords Green synthesis · 1,2,4-triazole derivatives · Antileishmanial activity · In silico studies · Docking on leishmanial MAPK

Supplementary information The online version of this article (https://doi.org/10.1007/s00044-018-2274-x) contains supplementary material, which is available to authorized users.

✉ Ahmed M. El-Saghier
el_saghier@yahoo.com

✉ Adnan A. Bekhit
adnbekhit@hotmail.com

[1] Chemistry Department, Faculty of Science, Sohag University, Sohag 82524, Egypt

[2] Pharmaceutical Chemistry Department, Faculty of Pharmacy, Kafrelsheikh University, Kafr El-Sheikh 33516, Egypt

[3] Pharmaceutical Chemistry Department, Faculty of Pharmacy, Alexandria University, Alexandria 21521, Egypt

[4] Pharmacy Program, Allied Health Department, College of Health Sciences, University of Bahrain, P.O. Box 32038, Zallaq, Bahrain

Introduction

Leishmaniasis is a protozoal and a dangerous disease that is common in tropical African regions, Southern Europe, Central and South America, the Middle East, and the Indian subcontinent (Khattab et al. 2017). According to WHO, it is classified as one of dangerous tropical protozoal diseases. Leishmaniasis is founded by obligate intracellular vector-borne parasites, which belong to genus *Leishmania* and family *Trypanosomatidae* (Shokri et al. 2017). Protozoan parasites of the genus *Leishmanial* cause a wide spectrum of diseases including visceral, cutaneous, mucocutaneous and diffused cutaneous leishmaniasis (Khattab et al. 2017). Cutaneous Leishmania (CL) is a parasitic infectious disease that affects the skin, cartilage and mucosa of the upper respiratory tract (Khattab et al. 2017). *L. major, L. tropica and L. aethiopica* are causative agents for CL (Salerno et al. 2014). Sodium stibogluconate, meglumine antimoniate, amphotericin B, miltefosine, pentamidine and paromomycin are drugs used for the treatment of leishmaniasis, but resistance, high cost and side effects have been reported almost for all the current therapeutic agents in addition to their toxicity (Alviano et al. 2012). To tackle this problem, new agents are urgently needed (Walker et al. 2012; Bekhit et al. 2015). Azoles especially triazoles are well known to have a broad spectrum of biological activities (Demirbas et al. 2004; Shams el-Dine and Hazzaa 1974; Cansiz et al. 2001; Misato et al. 1977; El-Kerdawy et al. 1989; Moustafa 2001; Sun et al. 2007; Shivarama Holla et al. 2003; Khanmohammadi et al. 2008). Furthermore, several reports showed that A (Papadopoulou et al. 2012), B (Girmenia 2009) and C (Mast et al. 2013) (Fig. 1) exhibited anti-leishmanial activity. Moreover, ravuconazole, albaconazole, and isavuconazole (triazole derivatives) are currently under investigation in clinical trials (Mindt et al. 2006).

As a continuation of our efforts to discover diverse chemotypes (Ibrahim et al. 2015) for potent antileishmanial agents (Atta et al. 2017; Bekhit et al. 2015; Birhan et al. 2014; Khattab et al. 2017), we aim at preparing new 1,2,4-triazole derivatives coupled with different amino acids. The synthetic process comprises green conditions, e.g., using lemon juice as green catalyst and aqueous medium as green solvent.

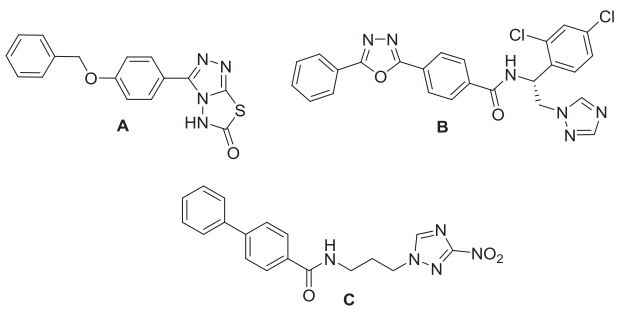

Fig. 1 Structures of lead antileishmania of 1,2,4-triazole moiety

Materials and methods

Chemistry

Melting points were determined in open-glass capillaries using a Griffin melting point apparatus and are all uncorrected. Infrared spectra (IR) were recorded on Perkine Elmer1430 infrared spectrophotometer. ^{1}HNMR and ^{13}CNMR were scanned on Jeol-400MHzNMR-spectrometer (DMSO-d6) and chemical shifts are given in d (ppm) down field from tetra methyl silane as internal standard. Micro analyses were performed on Vario El Fab-Nr elemental analyser. Mass spectra were determined on a Hewlett Packard 5988 spectrometer (Microanalysis Center, Cairo University, Egypt). Following up of the reactions as performed by thin-layer chromatography (TLC) on silica gel (60GF254)-coated glass plates and the spots were visualized by exposure to iodine Vapours or UV-lamp at 1254 nm for few seconds.

General procedure for the extraction of lemon juice

Fresh lemon (*Citrus limon*) was cut by using a knife and then pressed by hand using a presser to extract the juice; then juice was filtered through filter paper to remove solid material to obtain a clear juice that was used as a catalyst. The main ingredients of lemon juice are moisture (85%), carbohydrates (11.2%), citric acid (5–7%), protein (1%), vitamin C (0.5%), fat (0.9%), minerals (0.3%), fibres (1.6%), and some other organic acids.

Lemon juice is acidic in nature (pH ≈ 2–3) and its catalytic efficiency mainly came from the relatively higher percentage of citric acid (5–7%) compared to other acids. Lemon juice is previously reported to be used as active weak soluble catalyst (Patil et al. 2012; Pal et al. 2013).

General method for preparation of 2-amino-5(2-hydroxyphenyl)-1,2,4-triazole carboxylic acid 5a−k

An equimolar mixture of 2-hydroxy benzaldehyde/2-hydroxy acetophenone (0.01 mol), substituted amino acids (B-alanine, a-alanine, tryptophane, valine, aspartic acid, histadine, phenyl alanine and methonine, respectively) (0.01 mol), and thiosemicarbazide (0.01 mol) in solvent (15 mL water, containing 1−2 mL of ethanol) in the presence of lemon juice (2 mL) was mixed in a round-bottomed flask and the mixture was refluxed for the time needed to complete the reaction (2−3 h) (as monitored by TLC). After completion of the reaction, the mixture was cooled to room

temperature and the solid mass of the compounds was filtered and recrystallized from ethanol.

2-[3-Amino-5-(2-hydroxy-phenyl)-1,5-dihydro-[1,2,4]triazol-4-yl]-propionic acid (5a)

Yield (86%), off-white crystal, mp 238–240 °C, anal. Calcd. for $C_{11}H_{15}N_4O_3$ (Mr = 250.26): C, 52.58; H, 6.02; N, 22.30; O, 19.10. Found: C, 52.30; H, 6.09; N, 22.40; O, 20.21%. IR (KBr, cm^{-1}): 3502 (O–H), 3439 (O–H), 3314–3210 (NH_2), 3170 (NH), 3032 (C–H)$_{aromatic}$, 2983 (C–H)$_{aliphatic}$, 1616 (C=N), 1598 (COOasy), 1535 (COOsy), 1263 (Ph–O). ^{1}HNMR (400 MHz; δ ppm, d_6-DMSO: 2.52 (d, J = 4.69 Hz, 3H, CH_3), 2.95 (q, J = 4.75 Hz, 1H, CH−COOH), 3.78 (s, 1H, $CH_{triazole}$), 7.91 (s, 1H, NH, disappeared by D_2O), 6.79–7.90 (m, 4H, ArH), 8.10 (s, 1H, NH, disappeared by D_2O), 8.39 (s, 1H, OH, disappeared by D_2O), 9.88 (s, 1H, NH, disappeared by D_2O), 11.37 (s, 1H, OH, disappeared by D_2O), ^{13}CNMR (100 MHz; d_6-DMSO, δ ppm); 20.39 (CH_3), 35.74 (CH-COOH), 60.59 ($CH_{triazole}$), 116.80–140.84 (m, ArC), 156.91 (C=N), 178.41(C=O). MS (m/z^+, %): 249 (M^{-1}, 1.76%); 232 (4.76); 195 (100%); 178 (8.29); 120 (88.16); 107 (20.45); 91 (30.72).

2-[3-Amino-5-(2-hydroxy-phenyl)-5-methyl-1,5-dihydro-[1,2,4]triazol-4-yl]-propionic acid (5b)

Yield (87%), off-white crystal, mp 189–191 °C, anal. Calcd. for $C_{12}H_{17}N_4O_3$ (Mr = 265.59): C, 54.33; H, 6.46; N, 21.12; O, 18.19. Found: C, 54.23; H, 6.30; N, 21.22; O; 18.25 %. IR (KBr, cm^{-1}); 3552 (O–H), 3390 (O–H), 3289–3202 (NH_2), 3254 (NH), 3010 (C–H)$_{aromatic}$, 2991 (C–H)$_{aliphatic}$, 1641 (C=N), 1614 (COOasy), 1587 (COOsy), 1227 (Ph–O). ^{1}HNMR (400 MHz; d_6-DMSO, δ ppm); 2.22 (s, 3H, CH_3), 2.32 (d, J = 6.12 Hz, 3H, CH_3), 2.97(q, J = 6.40 Hz, 1H, CH−COOH), 6.86–7.54 (m, 4H, ArH), 8.02 (s, 1H, NH, disappeared by D_2O), 10.52(s_{broad}, 3H, NH_3, exchangeable by D_2O), 12.73 (s, 1H, OH, disappeared by D_2O). ^{13}CNMR (100 MHz; d_6-DMSO, ppm); 15.08 (CH_3), 24.55 (CH3), 36.42 (CH−COOH), 57.72 ($C_{triazole}$), 117–149.37 (m, ArC), 152.91 (C=N), 157.72 (C-OH), 180.95 (C=O). MS (m/z^+, %): 268 (M^{+2}, 100%); 251 (34.34); 210 (16.35); 195 (70%); 175 (6.92); 134 (61.52); 120 (39.45).

2-[3-Amino-5-(2-hydroxy-phenyl)-1,5-dihydro-[1,2,4]triazol-4-yl]-3-(1H-indol-3-yl)-propionic acid (5c)

Yield (81%), yellow crystal, mp 230–232 °C, anal. Calcd. for $C_{19}H_{19}N_5O_3$ (Mr = 365.39): C, 62.46; H, 5.24; N, 19.17; O, 13.14. Found: C, 61.99; H, 5.20; N, 19.41; O, 13.27%. IR (KBr, cm^{-1}); 3554 (O–H), 3413 (O–H), 3311–3200 (NH_2), 3171 (NH), 3142 (NH $_{indole}$), 3018 (C–H)$_{aromatic}$, 2989 (C–H)$_{aliphatic}$, 1629 (C=N), 1612 (COOasy), 1548 (COOsy), 1254 (Ph–O). ^{1}HNMR (400 MHz; d_6-DMSO, δ ppm): 2.84 (t, J = 14.47 Hz, 1H, CH−COOH), 3.10 (d, J = 14.93 Hz, 1H, CH_2), 3.76 (d, J = 15.04 Hz, 1H, CH_2), 5.51 (s, 1H, CHtriazole), 6.70 (s, 1H, CH indole), 6.72 (s, 1H, NH, disappeared by D2O), 6.70–7.83 (m, 8H, ArH), 7.85 (s, 1H, NH, disappeared by D_2O), 8.40 (s, 1H, OH, disappeared by D_2O), 10.14 (s, 1H, NH, disappeared by D_2O), 10.73 (s, 1H, NH $_{indole}$, disappeared by D_2O), 11.20 (s, 1H, OH, disappeared by D_2O). ^{13}CNMR (100 MHz; d_6-DMSO, δ ppm): 25.44 (CH_2), 52.36 (CH−COOH), 55.23 ($CH_{triazole}$), 107.35 (CH_{indole}), 111.81–140.65 (m, ArC and C of indole), 156.98 (C=N), 173.66 (C−OH), 178.48 (C=O).

2-[3-Amino-5-(2-hydroxy-phenyl)-5-methyl-1,5-dihydro-[1,2,4]triazol-4-yl]-3-(1H-indol-3-yl)-propionic acid (5d)

Yield (85%), off-white crystal, mp 220–222 °C, anal. Calcd. for $C_{20}H_{21}N_5O_3$ (Mr = 379.41): C, 63.31; H, 5.58; N, 18.46; O, 12.65. Found: C, 63.01; H, 5.21; N, 18.83; O, 12.95%. IR (KBr, cm^{-1}); 3542 (O–H), 3438 (O–H), 3313–3212 (NH_2), 3168 (NH), 3132 (NH_{indole}), 3014 (C–H)$_{aromatic}$, 2983 (C–H)$_{aliphatic}$, 1617 (C=N), 1600 (COOasy), 1534 (COOsy), 1263 (Ph–O). ^{1}HNMR (400 MHz; d_6-DMSO, δ ppm): 2.33 (s, 3H, CH_3), 3.11 (t, J = 3.96 Hz, 1H, CH−COOH), 3.34 (d, J = 4.08 Hz, 1H, CH_2), 3.66 (d, J = 3.81 Hz, 1H, CH_2), 6.84 (s,1H, CH_{indole}), 6.89 (s, 1H, NH, disappeared by D_2O), 6.90–7.91 (m, 8H, ArH), 8.12 (sbroad, 3H, NH_3, exchangeable by D_2O), 10.94 (s, 1H, NH_{indole}, disappeared by D_2O), 12.96 (s, 1H, OH, disappeared by D_2O). ^{13}CNMR (100 MHz; d_6-DMSO, δ ppm): 14.37 (CH_3), 24.43 (CH_2), 27.63 (CH−COOH), 55.03 ($C_{triazole}$), 109.40 (CH_{indole}), 111.82–136.80 (m, ArC and C of indole), 149.42 (C−NH), 157.90 (C=N), 172.30 (C−OH), 181.82 (C=O). MS (m/z^+, %): 379.10 (M, 0.1%); 192.10 (11.83%).

2-[3-Amino-5-(2-hydroxy-phenyl)-1,5-dihydro-[1,2,4]triazol-4-yl]-3-methyl-butyric acid (5e)

Yield (88%), off-white crystal, mp 247–249 °C, anal. Calcd. for $C_{13}H_{18}N_4O_3$ (Mr = 278.31): C, 56.10; H, 6.52; N, 20.13; O, 17.25. Found: C, 56.12; H, 6.30; N, 20.15; O, 17.42%. IR (KBr, cm^{-1}); 3542 (O–H), 3439 (O–H), 3319 (NH), 3177 (NH), 3022 (C–H)$_{aromatic}$, 2983 (C–H)$_{aliphatic}$, 1624 (C=N), 1612 (COOasy), 1537 (COOsy), 1273 (Ph–O). ^{1}H NMR (400 MHz; d_6-DMSO, δ ppm); 0.87 (d, J = 7.05 Hz, 3H, CH_3), 0.93 (d, J = 6.76 Hz, 3H, CH_3), 2.13 (m, 1H, CH−CH_3), 3.05 (d, J = 3.20 Hz, 1H, CH−COOH), 3.76 (s, 1H, $CH_{triazole}$), 6.80–7.25 (m, 4H, ArH), 7.93 (s, 1H, NH, disappeared by D_2O), 8.11 (s, 1H, OH, exchangeable by D_2O), 8.37 (s, 1H, NH, disappeared by D_2O), 9.98 (s, 1H, NH, disappeared by D_2O), 11.37 (s, 1H, OH,

disappeared by D_2O). ^{13}CNMR (100 MHz; d_6-DMSO, δ ppm): 17.74 (CH_3), 19.12 (CH_3), 29.42 (CH−CH_3), 47.87 (CH−COOH), 60.61 ($CH_{triazole}$), 121.47–133.95 (m, ArC), 158.48 (C=N), 167.85 (C−OH), 190.46 (C=O).

2-[3-Amino-5-(2-hydroxy-phenyl)-5-methyl-1,5-dihydro-[1,2,4]triazol-4-yl]-3-methyl-butyric acid (5f)

Yield (91%), off-white crystal, mp 195–197 °C, anal. Calcd. for $C_{14}H_{20}N_4O_3$ (Mr = 292.33): C, 57.52; H, 6.90; N, 19.17; O, 16.42. Found: C, 57.22; H, 7.10; N, 19.35; O, 16.14%. IR (KBr, cm^{-1}): 3498 (O–H), 3402 (O–H), 3291 (NH), 3120 (NH), 3022 (C–H)$_{aromatic}$, 2951 (C–H)$_{aliphatic}$, 1636 (C=N), 1608 (COOasy), 1508 (COOsy), 1244 (Ph–O). ^{1}H NMR (400 MHz; d_6-DMSO, δ ppm); 0.83 (d, J = 6.45 Hz, 3H, CH_3), 0.98 (d, J = 6.48 Hz, 3H, CH_3), 1.09 (s, 3H, CH_3), 2.29 (m, 1H, CH−CH_3), 3.00 (d, J = 4.67 Hz, 1H, CH–COOH), 6.66 (s, 1H, NH, disappeared by D_2O), 6.76–7.25 (m, 4H, ArH), 7.52, 7.62 (ss, 2H, NH, OH, disappeared by D_2O), 8.30 (s, 1H, OH, exchangeable by D_2O), 8.55 (s, 1H, NH, disappeared by D_2O). ^{13}CNMR (100 MHz; d_6-DMSO, δ ppm); 18.99 (CH_3), 19.11 (CH_3), 22.15 (CH_3), 32.23 (CH−CH_3), 49.05 (CH−COOH), 62.99 ($C_{triazole}$), 109.84–136.16 (m, ArC), 152.72 (C=N), 154.22 (C−OH), 176.11 (C=O).

2-[3-Amino-5-(2-hydroxy-phenyl)-1,5-dihydro-[1,2,4]triazol-4-yl]-3-(3H-imidazol-4-yl)-propionic acid (5g)

Yield (80%), brown crystal, mp 232–234 °C, anal. Calcd. for $C_{14}H_{16}N_6O_3$ (Mr = 316.32): C, 53.16; H, 5.10; N, 26.57; O, 15.17. Found: C, 53.30; H, 5.16; N, 26.27; O, 15.07%. IR (KBr, cm^{-1}); 3410 (O–H), 3398 (O–H), 3282 (NH), 3234 (NH), 3212 (NH), 3012 (C–H)$_{aromatic}$, 2988 (C–H)$_{aliphatic}$, 1648 (C=N), 1619 (COOasy), 1594 (COOsy), 1235 (Ph–O). ^{1}H NMR (400 MHz; d_6-DMSO, δ ppm); 3.44 (t, J = 3.75 Hz, 1H, CH−COOH), 4.06 (d, J = 3.96 Hz, 1H, CH_2), 4.28 (d, J = 4.16 Hz, 1H, CH_2), 5.25 (s, 1H, $CH_{triazole}$), 7.40, 8.58 (ss, 2H, $2CH_{imidazole}$), 6.85 (s, 1H, NH, disappeared by D_2O), 6.81–7.83 (m, 4H, ArH), 7.78 (s, 1H, OH, disappeared by D_2O), 8.98 (s, H, $NH_{imidazole}$, disappeared by D_2O), 9.82 (s, 1H, NH disappeared by D_2O), 11.24 (s, 2H, NH, OH, disappeared by D_2O). ^{13}CNMR (100 MHz; d_6-DMSO, δ ppm); 23.65 (CH_2), 32.96 (CH−COOH), 60.09 ($CH_{triazole}$), 115.12–132.05(m, ArC), 129.44, 141.32 (2CH of imidazole), 146.22 (C=N), 156.58 (C−OH), 177.45 (C=O).

2-[3-Amino-5-(2-hydroxy-phenyl)-5-methyl-1,5-dihydro-[1,2,4]triazol-4-yl]-3-(3H-imidazol-4-yl)-propionic acid (5h)

Yield (82%), orange crystal, mp 166–168 °C, anal. Calcd. for $C_{15}H_{18}N_6O_3$ (Mr = 330.32): C, 54.54; H, 5.49; N, 25.44; O, 14.53. Found: C, 54.54; H, 8.37; N, 25.49; O, 14.50%. IR (KBr, cm^{-1}); 3389 (O–H), 3372 (O–H), 3282–3204 (NH_2), 3243 (NH), 3022 (C–H)$_{aromatic}$, 2993 (C–H)$_{aliphatic}$, 1644 (C=N), 1614 (COOasy), 1591 (COOsy), 1229 (Ph–O). ^{1}H NMR (400 MHz; $CDCl_3$, δ ppm); 2.34 (s, 3H, CH_3), 2.40 (d, J = 4.37 Hz, 1H, CH_2), 2.61 (d, J = 4.56 Hz, 1H, CH_2), 3.92 (t, J = 4.28 Hz, 1H, CH−COOH), 6.50 (s_{broad}, 3H, NH_3, disappeared by D_2O), 6.97, 7.50 (ss, 2H, $2CH_{imidazole}$), 6.99–7.50 (m, 4H, ArH), 7.35 (s, 1H, NH, disappeared by D_2O), 8.75 (s, 1H, $NH_{imidazole}$, disappeared by D_2O), 10.68 (s, 1H, OH, disappeared by D_2O). ^{13}CNMR (100 MHz; $CDCl_3$, δ ppm); 19.66 (CH_3), 29.20 (CH_2), 50.20 (CH−COOH), 65.88 ($C_{triazole}$), 121.87–132.88 (m, ArC), 122.26,135.88 (2CH of imidazole), 158.27 (C=N), 160.46 (C−NH), 162.65 (C−OH), 186.92 (C=O).

2-[3-Amino-5-(2-hydroxy-phenyl)-1,5-dihydro-[1,2,4]triazol-4-yl]-3-phenyl-propionic acid (5i)

Yield (84%), brown crystal, mp 255–257 °C, anal. Calcd. for C17H18N4O3 (Mr = 326.35): C, 62.57; H, 5.56; N, 17.17; O, 14.71. Found: C, 62.10; H, 5.57; N, 17.57; O, 14.77%. IR (KBr, cm^{-1}); 3439 (O–H), 3374(O−H), 3312 (NH), 3136 (NH), 3015 (C–H)$_{aromatic}$, 2983 (C–H)$_{aliphatic}$, 2942 (CH2)$_{aliphatic}$, 1627 (C=N), 1602 (COOasy), 1534 (COOsy), 1262 (Ph–O). ^{1}HNMR (400 MHz; d_6-DMSO, δ ppm); 1.54 (d, J = 12.0 Hz, 1H, CH_2), 1.61 (d, J = 12.0 Hz, 1H, CH_2), 3.01 (t, J = 12.5 Hz, 1H, CH−COOH), 5.24 (s, 1H, $CH_{triazole}$), 6.81 (s, 1H, NH, disappeared by D_2O), 6.82–7.87 (m, 9H, ArH), 8.01 (s, 1H, NH, disappeared by D_2O), 8.39 (s, 1H, OH, exchangeable by D_2O), 10.24 (s, 1H, NH, disappeared by D_2O), 11.27 (s, 1H, OH, disappeared by D2O). ^{13}CNMR (100 MHz; d_6-DMSO, δ ppm); 18.97 (CH_2), 44.40 (CH−COOH), 56.52 ($CH_{triazole}$), 116.63–136.16 (m, 2ArC), 163.23 (C−OH), 178.51 (C=O).

2-[3-Amino-5-(2-hydroxy-phenyl)-5-methyl-1,5-dihydro-[1,2,4]triazol-4-yl]-4-methylsulfanyl-butyric acid(5j)

Yield (79%), yellow crystal, mp 173–175 °C, anal. Calcd. for $C_{14}H_{20}N_4O_3S$ (Mr = 324.40): C, 51.83; H, 6.21; N, 17.27; O, 14.80. Found: C, 51.34; H, 6.70; N, 17.31; O, 14.86%. IR (KBr, cm^{-1}); 3434 (O–H), 3302–3204 (NH_2), 3120 (NH), 3044 (C–H)$_{aromatic}$, 2998 (C–H)$_{aliphatic}$, 1634 (C=N), 1614 (COOasy), 1539 (COOsy), 1263 (Ph–O). ^{1}HNMR (400 MHz; d_6-DMSO, δ ppm); 2.46 (q, J = 6.00 Hz, 2H, CH_2), 2.54 (s, 3H, CH_3), 3.53 (t, J = 5.96 Hz, 2H, CH_2-S), 3.66 (s, 3H, CH_3-S), 4.06 (t, J = 6.12 Hz, 1H, CH−COOH), 6.76 (s, 1H, NH, disappeared by D_2O), 6.82 (s, 1H, NH, disappeared by D_2O), 6.83–7.58 (m, 4H, ArH), 7.22 (s, 1H, NH, disappeared by D_2O), 8.49 (s, 1H, OH, disappeared by D_2O), 13.07 (s, 1H, OH, disappeared by D_2O). ^{13}CNMR (100 MHz; d_6-DMSO, δ ppm); 14.32

(CH_3), 18.97 (CH_2), 31.91 (CH_3), 46.55 (S−CH_2), 56.51 (CH−COOH), 60.58 ($C_{triazole}$), 117.38–138.97 (m, ArC), 159.46 (C=N), 162.66 (C−OH), 174.37 (C=O).

2-[3-Amino-5-(2-hydroxy-phenyl)-1,5-dihydro-[1,2,4]triazol-4-yl]-succinic acid (5k)

Yield (83%), brown crystal, mp 180–182 °C, anal. Calcd. for $C_{12}H_{14}N_4O_5$ (Mr = 294.26): C, 48.98; H, 4.80; N, 19.04; O, 27.19. Found: C, 49.09; H, 4.54; N, 19.30; O, 27.08%. IR (KBr, cm^{-1}); 3427 (O–H), 3310–3204 (NH_2), 3108 (NH), 3022 $(C–H)_{aromatic}$, 2987(O–H), 2951 $(C–H)_{aliphatic}$, 1640 (C=N), 1614 (COOasy), 1539 (COOsy), 1261 (Ph–O). ^{1}H NMR (400 MHz; d_6-DMSO, δ ppm); 2.90 (t, J = 9.30 Hz, 1H, CH-COOH), 3.17 (d, J = 9.49 Hz, 1H, CH_2), 3.51 (d, J = 9.32 Hz, 1H, CH_2), 4.26 (s, 1H, $CH_{triazole}$), 6.83 (s, 1H, NH, disappeared by D_2O), 6.90–7.81 (m, 4H, ArH), 7.22 (s, 1H, NH, disappeared by D_2O), 7.40 (s, 1H, NH, disappeared by D_2O), 7.81 (s, 1H, OH, disappeared by D_2O), 8.41 (s, 1H, OH, disappeared by D_2O), 10.83 (s, 1H, OH, disappeared by D_2O). ^{13}CNMR (100 MHz; d_6-DMSO, δ ppm); 38.23 (CH_2), 57.22 (CH−COOH), 58.32 ($CH_{triazole}$), 116.57–135.88 (m, ArC), 158.27 (C−OH), 170.98 (C=O), 179.21 (C=O).

Biological screening

In vitro antileishmanial activity on Leishmanial major promastigotes

All the test compounds were dissolved in DMSO and were evaluated for their antileishmanial activity on *L. major* promastigotes as reported earlier (Bekhit et al. 2015; Atta et al. 2017).

In vivo acute toxicity testing

The most active compounds **5c**, **5d**, **5e** and **5f**, which showed promising antileishmanial activity, were tested for their oral acute toxicity in mice as reported earlier (Bekhit et al. 2015; Atta et al. 2017).

In silico study

Reverse docking experiments

The coordinates for MAPK (PDB code: 4QNY), trypanothione reductase (PDB code: 5EBK) *N*-myristoyltransferase (PDB code: 5G20) and *Lm*-PTR1 (PDB code: 2BFM) crystal structures were retrieved from the PDB. The prepared structures with Molecular Operating Environment (MOE) (Molecular Operating Environment (MOE 2016), Chemical Computing Group Inc.: Montreal, http://www.chemcomp/com) were adopted and used directly from our previous report (Atta et al. 2017).

The compounds were built and prepared by MOE. Generation of meaningful protonation states, energy minimization steps and calculation of partial charges were conducted as reported earlier (Atta et al. 2017). The prepared molecules were then saved as SD file for the docking experiments.

GOLD (version 5.2) (Hartshorn et al. 2007; Jones et al. 1995a, 1995b, 1997; Korb et al. 2009, 2012) was used for docking experiments employing ChemPLP scoring function. The docking parameters and settings were used as reported earlier (Atta et al. 2017). All graphical representations in Fig. 2 were rendered by MOE.

Physicochemical properties and pharmacokinetics profile predictions

The most active compounds **5c**, **5d**, **5e** and **5f** and their stereoisomers were tested for their drug-likeness, lead-likeness criteria and their pharmacokinetic profile was predicted using SwissADME (Daina et al. 2017) with its underlying methodologies to calculate descriptors for physicochemical parameters, drug-likeness parameters, and medicinal chemistry friendliness parameters.

Results and discussion

Chemistry

Reactions of amino acids to afford the synthesis of 1,2,4-triazole derivatives are well discussed in literature (Sachdeva et al. 2013b; Mali and Telvekar 2017; Blayo et al. 2011). The target compounds 2-amino-5-hydroxyphenyl-1,2,4-triazole carboxylic acid derivatives **5a**−**k** were prepared by one-pot multicomponent reaction approach via the reaction of an aromatic aldehyde/ketone (2-hydroxy benzaldehyde **1**/2-hydroxy acetophenone **2**), different L(*S*)-amino acids **3** (alanine, tryptophan, valine, histidine, phenyl alanine, methionine and aspartic acid) and thiosemicabazide **4** in the presence of lemon juice as a natural acidic catalyst in aqueous medium (13 mL H_2O: 2 mL ethanol) (Sachdeva et al. 2013a) with refluxing at 100 °C for 2−3 h (Scheme 1, Table 1).

The IR spectral data of 2-amino-5-hydroxyphenyl-1,2,4-triazole carboxylic acid derivatives **5a**−**k** showed a wide vibration band of (O–H) group situated in the range of 3391–3439 cm^{-1}, bands of NH_2 and NH groups appeared in the range (3289–3202)–(3314–3310) and 3169–3242 cm^{-1}, respectively. Also, intense band of (C=N) group was observed in the range 1633–1648 cm^{-1}. The vibration

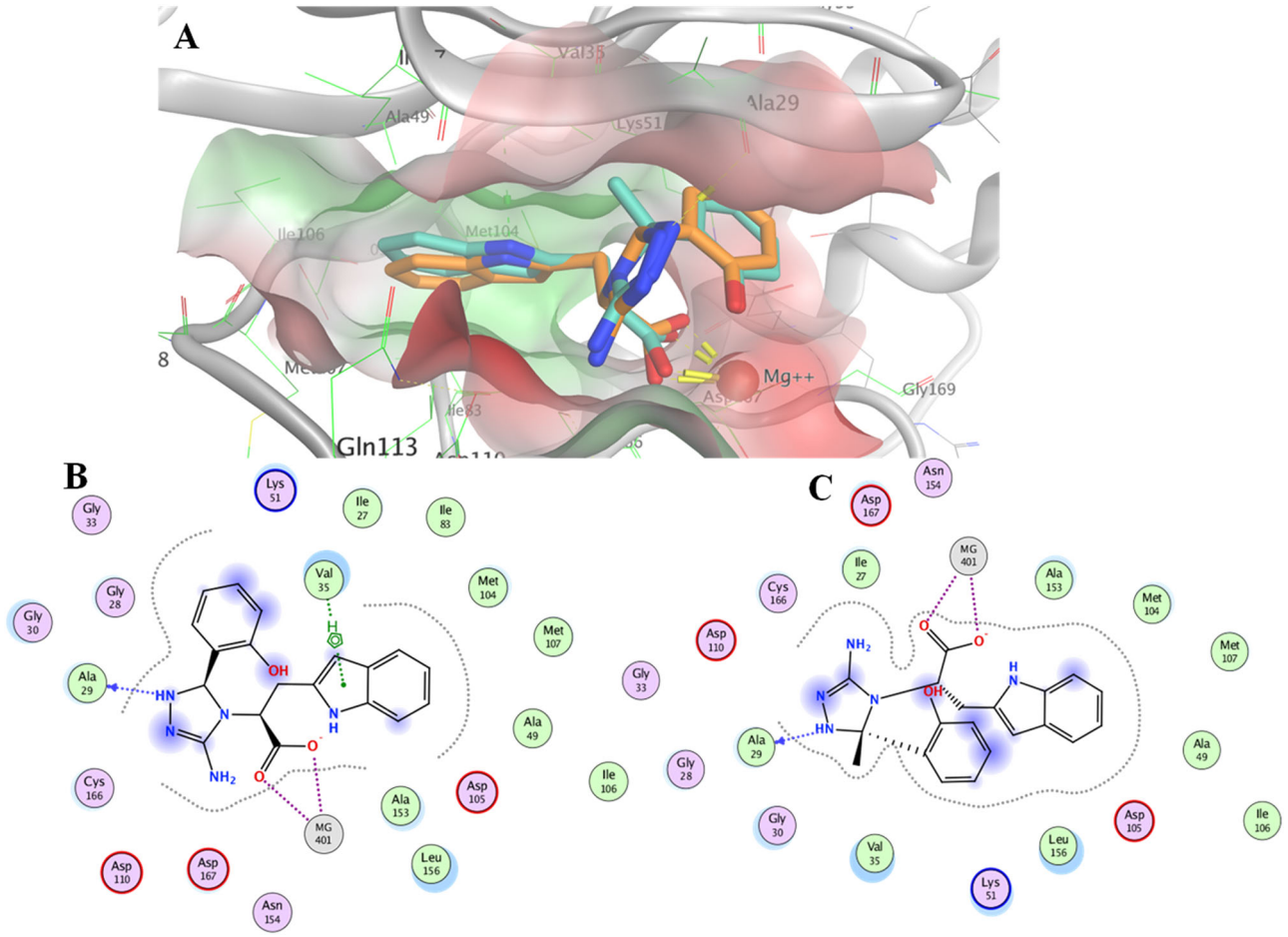

Fig. 2 **a** Overlay of docking poses of **5c** (orange sticks) and **5d** (cyan sticks) in 3D representation in the binding site of leishmanial MAPK. **b**, **c** are 2D interactions of **5c** and **5d**, respectively. The red and green colours of the surface representation of (**a**) indicate hydrophilic and hydrophobic areas, respectively. Polar hydrogen atoms were omitted for clarity

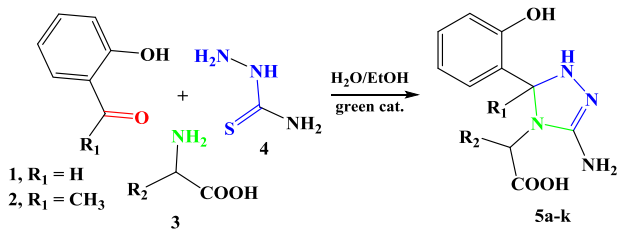

Scheme 1 Synthesis of 1,2,4-triazole derivatives **5a**–**k**

bands of (COO) sy and (COO) asy are distinct since they appear at a range between 1614–1589 and 1567–1494 cm^{-1}, respectively. We observed that when using tryptophan, histidine and aspartic acid, new bands corresponding to NH_{indole} group of compounds **5c**, **5d** at 3132, 3130 cm^{-1}, $NH_{imidazole}$ group of compounds **5g**, **5h** at 3212, 3178 cm^{-1} and $OH_{carboxylic}$ group of compounds **5k** at 2987 cm^{-1} had appeared, respectively.

The ^{1}HNMR spectral analysis of compound **5a** illustrated the existence of five deuterium exchangeable singlet signals which were attributed to NH_2, OH phenolic, NH and OH carboxylic groups at 7.91, 8.10, 8.39, 9.88 and 11.37 ppm, respectively. Also, doublet signals of CH_3 alanine group at 2.60 ppm were observed. Compound **5b** showed doublet signals of CH_3 alanine group at 2.22 ppm as well as CH_3 triazole group at 2.32 ppm. Also, three singlet signals related to NH, NH_3 and OH phenolic at 8.02, 10.52 and 12.73 ppm were observed respectively. Deshielded NH_3 signals were also noticed presumably due to occurrence of intramolecular hydrogen bond interaction with the carboxylic group. ^{13}C-NMR confirmed the structure of compounds **5a** and **5b** via demonstrating singlet signals corresponding to carbonyl group at 178 and 180 ppm, respectively. ^{1}H-NMR spectra of compounds **5c** and **5d** showed signals appearing at 10.73 and 10.94 ppm, respectively, relevant to NH_{indole} of tryptophan which disappeared by deuterium oxide. Also, there were two doublet signals owing to the CH_2 group at 2.85, 3.10 ppm for compound **5c**, and at 3.13, 3.33 ppm for compound **5d**.

^{1}H-NMR spectral analysis of compounds **5e** and **5f** reflect the presence of signals multiplicity, namely of two

Table 1 Characterization data of 2-amino-5-hydroxyphenyl-1,2,4-triazole carboxylic acid derivatives **5a**–**k**

Compound No.	R_1	R_2	Time (hrs)	Yield (%)
5a	H	$-CH_3$	2	86
5b	CH_3	$-CH_3$	2	87
5c	H	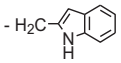	3	81
5d	CH_3	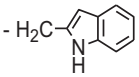	3	85
5e	H	$-CH(CH_3)_2$	2	88
5f	CH_3	$-CH(CH_3)_2$	2	91
5g	H	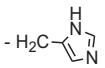	3	80
5h	CH_3	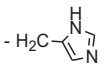	3	82
5i	H	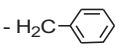	3	84
5j	CH_3	$-CH_2-CH_2-S-CH_3$	2	79
5k	H	$-CH_2-COOH$	2	83

CH_3 groups of valine at 0.87–0.93 and 0.83–0.98 ppm. Compounds **5g** and **5h** showed singlet signals appeared at 11.24 and 8.75 ppm corresponding to $NH_{imidazole}$ of histidine, respectively. Also two singlet signals of 2CH imidazole ring at 7.40, 8.58 ppm of compound **5g** and at 6.97, 7.35 ppm of compound **5h** were seen. ^{13}C-NMR spectra of compounds **5e**, **5f**, **5g** and **5h** showed the existence of new signals of valine and imidazole rings.

The ^{1}H-NMR spectrum analysis of compound **5i** illustrated that number of aromatic protons increased owing to the presence of phenyl group of phenyl alanine. However, compound **5j** contained five signals of aliphatic protons for $2CH_3$, $2CH_2$ and CH of methionine at δ (2.46, 3.51), (2.51, 3.66), and 4.86 ppm, respectively. Additionally, compound **5k** reflected the presence of a new singlet signal at 8.41 ppm relevant to the second OH carboxylic group of aspartic acid. ^{13}C-NMR spectra confirmed the chemical structure of these compounds. Besides, mass spectra confirmed the respective mass of our compounds. Examples of ^{1}H-NMR, ^{13}C-NMR and mass spectra can be found in the Supplementary Material. We also report method optimization for the synthesis in the Supplementary Material.

Biological screening

In vitro antileishmanial activity on Leishmanial major promastigotes

Compounds **5c**, **5e**, **5f**, **5i**, **5j** and **5k** showed IC_{50} values better than standard drugs miltefosine and comparable activity to amphotericin B deoxycholate against *L. Major* promastigote forms. The lead compound **5d** demonstrated higher activity with 200 folds better than miltefosine. Furthermore, compounds **5a**, **5b**, **5g** and **5h** showed lower IC_{50} values than amphotericin B and more than miltefosine against *L. major* promastigotes (Table 2).

The effect of varying R_1 between H (from 2-hydroxy benzaldehyde) and CH_3 (from 2-hydroxy acetophenone) on the antileishmanial activity appeared to be minimum. However, variation of R_2 via reacting different amino acids

showed obvious change in activity. For instance, compounds (**5c** and **5d**) that are reaction products of tryptophan amino acid showed the highest antileishmanial activity among other amino acid products. Similarly, reaction products of valine amino acid (**5e** and **5f**) demonstrated the uppermost antileishmanial activity. On the other hand, reaction products of alanine (**5a** and **5b**) and histidine (**5g** and **5h**) showed the lowest antileishmanial activity among the synthesized compounds. Generally, from such structure −activity relationship (SAR) observations one can conclude that antileishmanial activity favours more hydrophobic moiety with certain topology like isopropyl and indolyl groups, while disfavouring smaller or polar groups like methyl or imidazolyl groups, respectively. One factor to explain that is the nature and size features of the pocket accommodating R_2 group in the binding site of the possible putative target(s). This point can be rationalized in the docking section afterwards.

Table 2 Antipromastigote activity (IC_{50}) of the synthesized compounds

Compound	IC_{50}[a] values (μg/mL)
5a	1.0642 ± 0.12
5b	1.6484 ± 0.16
5c	0.0516 ± 0.28
5d	0.0312 ± 0.21
5e	0.0866 ± 0.04
5f	0.0484 ± 0.06
5g	1.1142 ± 0.14
5h	1.6249 ± 0.28
5i	0.8644 ± 0.04
5j	0.4662 ± 0.05
5k	0.8668 ± 0.02
Miltefosine	3.1924 ± 0.14
Amphotericin B deoxycholate	0.0472 ± 0.02

[a]IC_{50}: values indicate the effective concentration of a compound required to achieve 50% growth inhibition in μg/mL. Values are means of at least three experiments

In vivo acute toxicity testing

The most active antileishmanial compounds, **5c**, **5d**, **5e** and **5f**, were tested for their toxicity in mice. The experimental mice did not show any toxicity signs after treatment with the test compounds. There was no significant difference in the weight of the mice and no death cases were recorded during 3 days of observation post administration of the test compounds (data not shown). The test compounds were well tolerated by the experimental animals orally up to 250 mg/kg.

In silico study

Reverse docking experiment

To pinpoint a possible putative target for our compounds against *Leishmania*, we performed a reverse docking approach against some known leishmanial targets reported in literature (Rajasekaran and Chen 2015). We examined the in silico binding affinities (i.e. docking fitness) of the most active compounds **5c**, **5d**, **5e** and **5f** and their stereoisomers on the following novel targets for *Leishmania* species (Rajasekaran and Chen 2015): (a) Mitogen-activated protein kinase (MAPK—PDB code: 4QNY) as an example of protein kinase; (b) Trypanothione reductase (PDB code: 5EBK) as an example in Thiol metabolism; (c) *N*-myristoyltransferase (PDB code: 5G20) as an example in vital signal transduction; and (d) *Leishmania major* pteridine reductase *Lm*-PTR1 (PDB code: 2BFM) as an example in pteridine metabolism. Since all compounds are coupling products of L(*S*)-amino acids, they presumably show a mixture of both *R* and *S* absolute configuration at only one stereogenic centre (carbon number 5 of the triazolyl moiety), while the other stereogenic centre (carbon

Table 3 Reverse docking approach of the most active compounds against novel targets of *Leishmania*

Leishmanial targets	PDB	Docking fitness (SD[a])							
		5c (R)[b]	5c (S)	5d (R)	5d (S)	5e (R)	5e (S)	5f (R)	5f (S)
Lm-PTR1	2BFM	68.46 (1.02)	66.11 (5.35)	62.81 (0.21)	62.3 (0.50)	56.52 (4.04)	55.18 (0.52)	59.12 (1.02)	51.74 (0.08)
N-myristoyltransferase	5G20	66.31 (0.75)	66.23 (0.01)	61.21 (1.58)	64.06 (0.14)	50.3 (0.36)	49.78 (1.24)	47.31 (1.48)	49.2 (1.47)
MAPK	4QNY	80.58 (1.36)	84.46 (1.87)	75.43 (0.73)	76.37 (2.63)	65.84 (0.09)	62.56 (2.67)	53.76 (2.61)	60.64 (0.03)
Trypanothione reductase	5EBK	63.1 (1.44)	53.53 (0.02)	57.66 (0.44)	61.55 (0.14)	50.24 (1.95)	46.05 (0.27)	44.71 (0.03)	43.69 (0.33)

The fitness values are for best-scored poses

[a]SD is the standard deviation of three consecutive runs. The docking score is expressed as fitness of ChemPLP scoring function of GOLD (v 5.2)

[b]The absolute configuration denoted is for carbon number 5 of the triazole group

number 2 of propionic/butyric acid derivative) will remain (*S*). Therefore, we state the absolute configuration for our compounds, e.g., **5c** (*S*), **5c** (*R*), etc., denoting the absolute configuration of carbon number 5 of the triazolyl moiety only, as mentioned in Table 3.

The docking results (Table 3) showed that the most active compounds **5c** and **5d** displayed the highest affinity towards MAPK among the aforementioned targets. In addition, all the docked compounds **5c**, **5d**, **5e** and **5f** demonstrated preferable in silico affinity against MAPK compared to other targets. Only exception can be observed for **5f** (*R*) where it showed better preference to *Lm*-PTR1. Generally, this presumably points to MAPK as a possible putative target for our compounds and, therefore, further in silico investigation concerning this enzyme was carried out.

MAPKs are crucial regulators of differentiation and cell proliferation in many eukaryotes (Rajasekaran and Chen 2015). Only few reports on targeting the leishmanial MAPK are available (Rajasekaran and Chen 2015). They designate that MAPK is essential for the growth of amastigote and could be investigated as a drug target (Rajasekaran and Chen 2015; Naula et al. 2005).

The most active compound **5d** showed high affinity binding to the binding site of MAPK. Its docking pose appeared to show various types of interaction. For instance, H-bonding interactions of N1 of triazolyl group with Ala 29 can be seen (Fig. 2). Also, its carboxylate group appeared to chelate with the metal ion Mg^{2+}. Besides, the indolyl group is observed to be packed between Ala 49, Met 104, Ile 106 and Met 107, highlighting favourable hydrophobic interactions. However, hydroxyl phenyl group showed limited access to Gly 28 forming hydrophobic interaction while the major topology of it is solvent exposed. Like **5d**, **5c** reproduced the key H-bonding interactions with the backbone of Ala 29, the chelation with Mg^{2+} metal ion and the other hydrophobic interactions. This can be observed from the optimum overlay of the docking poses of **5c** and **5d**, as shown in Fig. 2. However, the extra 5-methyl group of **5d** appeared to access more hydrophobic region comprised by Gly 30 and Val 35 residues.

Rationalizing the SAR observed in the in vitro antileishmanial section, one can inspect that R_2 group is generally packed in a sub-pocket formed by the residues Ala 49, Met 104, Ile 106 and Met 107. Such sub-pocket appeared to accommodate optimally indolyl group of **5c** and **5d** (Fig. 2a) and presumably capable to accommodate isopropyl group of **5e** and **5f**. However, binding event to such sub-pocket would not benefit from much smaller groups like methyl or imidazolyl for (**5a** and **5b**) and (**5g** and **5h**), respectively.

Based on our analysis to the docking poses of different stereoisomers of our compounds, we did not observe dramatic changes in the docking fitness between the respective **5d** and **5e** stereoisomers, while **5c** and **5f** showed minor differences. This observation is consistent with other screened leishmanial targets as well (Table 3). This roughly concludes that stereoisomerism at carbon number 5 of the triazolyl group does not appear to be crucial for antileishmanial activity.

Physicochemical properties and pharmacokinetics profile predictions

The aim of this part is to test the drug-likeness, lead-likeness criteria and to predict the pharmacokinetic profile of the most active compounds **5c**, **5d**, **5e** and **5f** and their stereoisomers. Generally, such predictions and metrics do not provide an absolute guarantee that a compound would be an optimum drug for an illness. Nevertheless, compounds that do not succeed the drug-likeness criteria often do not thrive to be an efficient clinical candidate due to poor bioavailability, adverse effects or other concerns. We used the automated SwissADME (Daina et al. 2017) server for such calculations and predictions.

Drug-likness parameters section (Table 4) evaluates qualitatively the chance for a molecule to become an oral drug with respect to bioavailability. Drug-likeness concept was basically established from structural or physicochemical inspections of development compounds advanced enough to be considered oral drug candidates. Here in our study we demonstrate some parameters calculated by SwissADME tool namely, Lipinski violations, Veber violations and Bioavailability Score.

Lipinski violations parameter counts the number of violations of the pioneer rule-of-five. Lipinski rule-of-five can be summarized as a compound to be orally bioavailable only if one violation of the following physicochemical properties conditions can be tolerable: lipophilicity (logP) ≤ 5, molecular weight ≤ 500, number of hydrogen bond donors ≤ 5 and number of hydrogen bond acceptors ≤ 10. A summary of such properties is shown in Table 4.

Nevertheless, Lipinski rule focusses on only physicochemical properties of the compounds; additional efforts (Ghose et al. 1999; Veber et al. 2002; Egan et al. 2000; Muegge et al. 2001)—such as Veber (Veber et al. 2002) violations parameter—are trying to encounter relevant structural properties to oral bioavailability such as topological polar surface area (TPSA) and number of rotatable bonds (NRB). Veber violation parameter counts the number of violations of Veber rule summarized as: NRB ≤ 10 and TPSA ≤ 140 $Å^2$. However, since physicochemical properties that manage the bioavailability and permeability of negatively charged compounds at pH 6−7 diverge from those that govern bioavailability of uncharged or positively charged compounds at same pH (Daina et al. 2017), we considered the "Bioavailability Score" (Martin 2005) of

Table 4 In silico predictions of the physicochemical, drug-likeness and medicinal chemistry friendliness parameters for the most active compounds

Physicochemical parameters									
Compound	Mwt	NRB	NHBA	NHBD	TPSA	XLOGP3	ESOL Log S	ESOL Sol. (mg/mL)	ESOL Class
5c	365.38	5	4	4	129.8	2.34	−3.65	0.08	Soluble
5d	379.4	5	4	4	129.8	2.52	−3.84	0.05	Soluble
5e	278.3	4	4	3	114.01	1.55	−2.49	0.89	Soluble
5f	292.33	4	4	3	114.01	1.74	−2.69	0.6	Soluble

Drug-likeness parameters				Medicinal chemistry friendliness parameters		
Compound	Lipinski violations	Veber violations	Bioavailability Score	PAINS alerts	Brenk alerts	Lead-likeness violations
5c	0	0	0.55	1	0	1
5d	0	0	0.55	1	0	1
5e	0	0	0.55	1	0	0
5f	0	0	0.55	1	0	0

The calculations performed using SwissADME

Mwt molecular weight, *NRB* number of rotatable bonds, *NHBA* number of hydrogen-bond acceptor, *NHBD* number of hydrogen bond donor, *TPSA* topological polar surface area, *XlogP3* a lipophilicity descriptor (logarithm of compound partition coefficient between n-octanol and water) calculated by the XLOGP program (Cheng et al. 2007), *ESOL Log S* a solubility descriptor (logarithm of solubility) calculated according to the ESOL model (Delaney 2004), *ESOL Class* log S scale, insoluble < −10 < poorly soluble < −6 < moderately soluble < −4 < soluble < −2 < very soluble < 0 < highly soluble, *PAINS* pan-assay interference compounds

Table 5 In silico pharmacokinetics parameters calculated by SwissADME

Pharmacokinetics parameters								
Compound	GIA	BBB permeation	P-gp substrate	CYP1A2 inhibition	CYP2C19 inhibition	CYP2C9 inhibition	CYP2D6 inhibition	CYP3A4 inhibition
5c (S)	High	No	Yes	No	No	No	No	No
5c (R)	High	No	Yes	No	No	No	No	No
5d (S)	High	No	Yes	No	No	No	No	No
5d (R)	High	No	Yes	No	No	No	No	No
5e (R)	Low	No	No	No	No	No	No	No
5e (S)	Low	No	No	No	No	No	No	No
5f (R)	High	No	No	No	No	No	No	No
5f (S)	High	No	No	No	No	No	No	No

GIA human gastrointestinal absorption, *BBB permeation* blood−brain barrier permeation, *P-gp* permeability glycoprotein

CYP1A2, CYP2C19, CYP2C9, CYP2D6 and CYP3A4 are the five major isoforms of cytochromes P450 (CYP)

SwissADME. Bioavailability Score is formulated as the likelihood that a compound will have >10% bioavailability in rat or measurable Caco-2 permeability. The score is 0.11 for anions for which TPSA is >150 Å^2, 0.56 if TPSA is between 75 and 150 Å^2, and 0.85 if TPSA is <75 Å^2. For the remaining compounds, Bioavailability Score is 0.55 if it passes Lipinski rule-of-five and 0.17 if it fails (Martin 2005). Bioavailability Score also identifies poorly- and well-absorbed compounds tested in humans. Interestingly, all four compounds and their stereoisomers showed promising bioavailability score without any violations of Lipinski or Veber rules. This together with the high GIA (Table 5) and good solubility (Table 4) emphasize the elevated chance of these compounds to possess high oral bioavailability and drug-likeness.

Medicinal chemistry friendliness parameters section (Table 4) gives support to early discover any possible artifacts in the discovery process of drug candidates. For instance, all the four compounds and their stereoisomers are considered safe according to Brenk (Brenk et al. 2008) structural alert. Brenk alert consists in a list of 105 fragments identified to be putatively toxic, chemically reactive, metabolically unstable or to bear properties responsible for poor pharmacokinetics. However, all compounds showed only one PAINS (pan-assay interference compounds) (Baell and Holloway 2010) alert which is the presence of phenolic

Mannich base substructure. This means that the compounds' chemical structure may possess an interfering substructure that can have a potent response in protein assays irrespective of the protein target. However, we expect that the influence of such PAINS substructure is minimal since the antileishmanial activity quantified in our study depends mainly on the promastigote viability which is indicated by the catalytic conversion of Alamar blue® (blue and non-fluorescent) to resorufin (pink and highly fluorescent) (Bekhit et al. 2015; Atta et al. 2017) rather than specific protein photometric assay.

Another parameter of medicinal chemistry parameters is lead-likeness. Lead-likeness concept is comparable to drug-likeness, yet centring on physicochemical borders defining a good lead, i.e. a molecular entity appropriate for further optimization (Daina et al. 2017). Basically, leads would undergo chemical alterations which would most likely enhance the size and lipophilicity features (Hann and Keseru 2012). Consequently, leads are required to be smaller and less hydrophobic than drug-like molecules. We used the lead-likeness parameter of SwissADME which is a rule-based method (Teague et al. 1999).

Based on lead-likeness violations parameter, one can declare that compounds **5c**, **5d** and their stereoisomers are potential candidates for drug discovery, while **5e**, **5f** and their stereoisomers are potential candidates for further lead optimization.

Pharmacokinetics parameters section (Table 5) employing specialized models assesses individual ADME behaviours of the four compounds and their stereoisomers. The predictions for passive human gastrointestinal absorption (GIA) and blood−brain barrier (BBB) permeation both extracted from the readout of the BOILED-Egg model (Daina and Zoete 2016; Daina et al. 2017). All four compounds and their stereoisomers showed high gastrointestinal absorption, with exception of **5e** stereoisomers which showed low GIA. This can be compensated by other parameters for drug-likeness prediction (Table 4) which assumes that all compounds would demonstrate acceptable oral bioavailability and drug-likeness properties. Fortunately, all these compounds do not qualify to be permeable through BBB, and hence, they expected to be with low incidence for central nervous system (CNS) adverse effects.

P-gp substrate parameter gives information about a compound being substrate or non-substrate of the permeability glycoprotein (P-gp) (Daina et al. 2017). P-gp is suggested to be the most important member among ATP-binding cassette transporters or ABC-transporters. P-gp is a key to judge active efflux through biological membranes, for instance to protect the CNS from xenobiotics (Szakacs et al. 2008; Daina et al. 2017). Although not all our compounds being substrates for P-gp (e.g., **5e** and **5f** in Table 5), the chance for CNS adverse effects is minimum due to low BBB permeation.

Having information about interaction of compounds with the cytochromes P450 (CYP) superfamily is of great importance. This superfamily of isoenzymes is the main actor in drug elimination through metabolic biotransformation (Testa and Kraemer 2007). It has been estimated that 50–90% of therapeutic molecules are substrate of five major isoforms (CYP1A2, CYP2C19, CYP2C9, CYP2D6, CYP3A4) (Wolf et al. 2000; Di 2014; Daina et al. 2017). Inhibition of these isoenzymes is undoubtedly one main source of pharmacokinetics-related drug−drug interactions (Hollenberg 2002; Huang et al. 2008) leading to toxic or adverse effects. Interestingly, all our investigated compounds did not show inhibition of any CYP five major isoforms (Table 5), indicating low incidence of drug−drug interactions.

Conclusions

The objectives of the present study were to synthesize and investigate the antileishmanial activities of some amino acids hybrids with 1,2,4-triazole derivatives. The in vitro *L. major* antipromastigote activity demonstrated that all synthesized compounds **5c**–**5k** showed better antileishmanial activity than standard drugs miltefosine. Particularly, the most active compound **5d** exhibited 200 folds more antileishmanial activity than miltefosine. Interestingly, compounds **5c**, **5d**, **5e** and **5f** demonstrated promising antileishmanial activity comparable to amphotericin B deoxycholate. Furthermore, compounds **5a**, **5b**, **5g** and **5h** showed lower antileishmanial activity than amphotericin B and more than miltefosine against *L. major* promastigotes. Reverse docking approach pinpointed MAPK as a putative antileishmanial target and the mode of action of the most active compounds was rationalized. This highlights the importance of further in vitro molecular investigations on leishmanial MAPK via vast biophysical techniques in the near future. Toxicity studies for the most active compounds indicated their safety via oral and parenteral routes up to 250 and 100 mg/kg, respectively. Also, acceptable in silico predictions of drug-likeness and pharmacokinetics profile were elaborated.

Acknowledgements The authors acknowledge Prof. Frank Boeckler (Lab. of Molecular Design and Pharmaceutical Biophysics, Eberhard Karls University of Tuebingen) for granting access to MOE and GOLD tools.

Compliance with ethical standards

Conflict of interest The authors declare that they have no conflict of interest

Ethical approval The protocols used in this study followed the guidelines set in "The Guide for the Care and Use of Laboratory Animals", and got approval from the ACUC, Faculty of Pharmacy, Alexandria University, Project No. 22 at 22/5/2013 and ACUC17/18.

References

Alviano DS, Barreto AL, Dias Fde A, Rodrigues Ide A, Rosa Mdo S, Alviano CS, Soares RM (2012) Conventional therapy and promising plant-derived compounds against trypanosomatid parasites. Front Microbiol 3:283. https://doi.org/10.3389/fmicb.2012.00283

Atta KFM, Ibrahim TM, Farahat OOM, Al-Shargabi TQ, Marei MG, Bekhit AA, El Ashry ESH (2017) Synthesis, modeling and biological evaluation of hybrids from pyrazolo[1,5c]pyrimidine as antileishmanial agents. Future Med Chem 9(16):1913–1929. https://doi.org/10.4155/fmc-2017-0120

Baell JB, Holloway GA (2010) New substructure filters for removal of pan assay interference compounds (PAINS) from screening libraries and for their exclusion in bioassays. J Med Chem 53 (7):2719–2740. https://doi.org/10.1021/jm901137j

Bekhit AA, Hassan AM, Abd El Razik HA, El-Miligy MM, El-Agroudy EJ, Bekhit Ael D (2015) New heterocyclic hybrids of pyrazole and its bioisosteres: design, synthesis and biological evaluation as dual acting antimalarial-antileishmanial agents. Eur J Med Chem 94:30–44. https://doi.org/10.1016/j.ejmech.2015.02.038

Birhan YS, Bekhit AA, Hymete A (2014) Synthesis and antileishmanial evaluation of some 2,3-disubstituted-4(3H)-quinazolinone derivatives. Org Med Chem Lett 4(1):10. https://doi.org/10.1186/s13588-014-0010-1

Blayo A-L, Brunel F, Martinez J, Fehrentz J-A (2011) Synthesis of various chiral 1,2,4-triazole-containing α-amino acids from aspartic or glutamic acids. Eur J Org Chem 2011(23):4293–4297. https://doi.org/10.1002/ejoc.201100611

Brenk R, Schipani A, James D, Krasowski A, Gilbert IH, Frearson J, Wyatt PG (2008) Lessons learnt from assembling screening libraries for drug discovery for neglected diseases. ChemMedChem 3(3):435–444. https://doi.org/10.1002/cmdc.200700139

Cansiz A, Servi S, Koparir M, Altintas M, Digrak M (2001) Synthesis and biological activities of some Mannich bases of 5-(2-furyl)-1, 2, 4-triazole-3-thiones. J Chem Soc Pak 23(4):237–239

Cheng T, Zhao Y, Li X, Lin F, Xu Y, Zhang X, Li Y, Wang R, Lai L (2007) Computation of octanol-water partition coefficients by guiding an additive model with knowledge. J Chem Inf Model 47 (6):2140–2148. https://doi.org/10.1021/ci700257y

Daina A, Michielin O, Zoete V (2017) SwissADME: a free web tool to evaluate pharmacokinetics, drug-likeness and medicinal chemistry friendliness of small molecules. Sci Rep 7:42717. https://doi.org/10.1038/srep42717

Daina A, Zoete V (2016) A boiled-egg to predict gastrointestinal absorption and brain penetration of small molecules. ChemMedChem 11(11):1117–1121. https://doi.org/10.1002/cmdc.201600182

Delaney JS (2004) ESOL: estimating aqueous solubility directly from molecular structure. J Chem Inf Comput Sci 44(3):1000–1005. https://doi.org/10.1021/ci034243x

Demirbas N, Karaoglu SA, Demirbas A, Sancak K (2004) Synthesis and antimicrobial activities of some new 1-(5-phenylamino-[1,3,4]thiadiazol-2-yl)methyl-5-oxo-[1,2,4]triazole and 1-(4-phenyl-5-thioxo-[1,2,4]triazol-3-yl)methyl-5-oxo- [1,2,4]triazole derivatives. Eur J Med Chem 39(9):793–804. https://doi.org/10.1016/j.ejmech.2004.06.007

Di L (2014) The role of drug metabolizing enzymes in clearance. Expert Opin Drug Metab Toxicol 10(3):379–393. https://doi.org/10.1517/17425255.2014.876006

Egan WJ, Merz Jr. KM, Baldwin JJ (2000) Prediction of drug absorption using multivariate statistics. J Med Chem 43 (21):3867–3877

El-Kerdawy M, Eisa H, Barghash A, Marouf A (1989) Synthesis and some chemical behaviour of certain substituted thiosemicarbazides. J Chin Chem Soc 36:347–351. https://doi.org/10.1002/jccs.198900048

Ghose AK, Viswanadhan VN, Wendoloski JJ (1999) A knowledge-based approach in designing combinatorial or medicinal chemistry libraries for drug discovery. 1. A qualitative and quantitative characterization of known drug databases. J Comb Chem 1 (1):55–68

Girmenia C (2009) New generation azole antifungals in clinical investigation. Expert Opin Investig Drugs 18(9):1279–1295. https://doi.org/10.1517/13543780903176407

Hann MM, Keseru GM (2012) Finding the sweet spot: the role of nature and nurture in medicinal chemistry. Nat Rev Drug Discov 11(5):355–365. https://doi.org/10.1038/nrd3701

Hartshorn MJ, Verdonk ML, Chessari G, Brewerton SC, Mooij WT, Mortenson PN, Murray CW (2007) Diverse, high-quality test set for the validation of protein-ligand docking performance. J Med Chem 50(4):726–741. https://doi.org/10.1021/jm061277y

Hollenberg PF (2002) Characteristics and common properties of inhibitors, inducers, and activators of CYP enzymes. Drug Metab Rev 34(1−2):17–35. https://doi.org/10.1081/DMR-120001387

Huang SM, Strong JM, Zhang L, Reynolds KS, Nallani S, Temple R, Abraham S, Habet SA, Baweja RK, Burckart GJ, Chung S, Colangelo P, Frucht D, Green MD, Hepp P, Karnaukhova E, Ko HS, Lee JI, Marroum PJ, Norden JM, Qiu W, Rahman A, Sobel S, Stifano T, Thummel K, Wei XX, Yasuda S, Zheng JH, Zhao H, Lesko LJ (2008) New era in drug interaction evaluation: US Food and Drug Administration update on CYP enzymes, transporters, and the guidance process. J Clin Pharmacol 48(6):662–670. https://doi.org/10.1177/0091270007312153

Ibrahim TM, Bauer MR, Dorr A, Veyisoglu E, Boeckler FM (2015) pROC-chemotype plots enhance the interpretability of benchmarking results in structure-based virtual screening. J Chem Inf Model 55(11):2297–2307. https://doi.org/10.1021/acs.jcim.5b00475

Jones G, Willett P, Glen RC (1995a) A genetic algorithm for flexible molecular overlay and pharmacophore elucidation. J Comput-Aided Mol Des 9(6):532–549

Jones G, Willett P, Glen RC (1995b) Molecular recognition of receptor sites using a genetic algorithm with a description of desolvation. J Mol Biol 245(1):43–53

Jones G, Willett P, Glen RC, Leach AR, Taylor R (1997) Development and validation of a genetic algorithm for flexible docking J Mol Biol 267(3):727–748. https://doi.org/10.1006/jmbi.1996.0897

Khanmohammadi H, Abnosi MH, Hosseinzadeh A, Erfantalab M (2008) Synthesis, biological and computational study of new Schiff base hydrazones bearing 3-(4-pyridine)-5-mercapto-1,2,4-triazole moiety. Spectrochim Acta Mol Biomol Spectrosc 71 (4):1474–1480. https://doi.org/10.1016/j.saa.2008.05.003

Khattab SN, Haiba NS, Asal AM, Bekhit AA, Guemei AA, Amer A, El-Faham A (2017) Study of antileishmanial activity of 2-aminobenzoyl amino acid hydrazides and their quinazoline derivatives. Bioorg Med Chem Lett 27(4):918–921. https://doi.org/10.1016/j.bmcl.2017.01.003

Korb O, Stutzle T, Exner TE (2009) Empirical scoring functions for advanced protein-ligand docking with PLANTS. J Chem Inf Model 49(1):84–96. https://doi.org/10.1021/ci800298z

Korb O, Ten Brink T, Victor Paul Raj FR, Keil M, Exner TE (2012) Are predefined decoy sets of ligand poses able to quantify scoring function accuracy? J Comput Aided Mol Des 26(2):185–197. https://doi.org/10.1007/s10822-011-9539-5

Mali DA, Telvekar VN (2017) Synthesis of triazolidines and triazole using DMAP. Synth Commun 47(4):324–329. https://doi.org/10.1080/00397911.2016.1263338

Martin YC (2005) A bioavailability score. J Med Chem 48(9):3164–3170. https://doi.org/10.1021/jm0492002

Mast N, Zheng W, Stout CD, Pikuleva IA (2013) Antifungal azoles: structural insights into undesired tight binding to cholesterol-metabolizing CYP46A1. Mol Pharmacol 84(1):86–94. https://doi.org/10.1124/mol.113.085902

Mindt TL, Struthers H, Brans L, Anguelov T, Schweinsberg C, Maes V, Tourwe D, Schibli R (2006) "Click to chelate": synthesis and installation of metal chelates into biomolecules in a single step. J Am Chem Soc 128(47):15096–15097. https://doi.org/10.1021/ja066779f

Misato T, Ko K, Honma Y, Konno K, Taniyama E (1977) JP 77-25028 (A01N9/12). Chem Abstr 87:147054a

Molecular Operating Environment MOE (2016), Chemical Computing Group Inc.: Montreal, http://www.chemcomp/com

Moustafa HM (2001) Synthesis and reactions of new fused heterocycles derived from 3-(o-Aminophenyl)-4-amino-5-mercapto-1, 2, 4-triazole. Synth Comm 31(1):97–109

Muegge I, Heald SL, Brittelli D (2001) Simple selection criteria for drug-like chemical matter. J Med Chem 44(12):1841–1846

Naula C, Parsons M, Mottram JC (2005) Protein kinases as drug targets in trypanosomes and Leishmania. Biochim Biophys Acta 1754(1−2):151–159. https://doi.org/10.1016/j.bbapap.2005.08.018

Papadopoulou MV, Bloomer WD, Rosenzweig HS, Chatelain E, Kaiser M, Wilkinson SR, McKenzie C, Ioset JR (2012) Novel 3-nitro-1H-1,2,4-triazole-based amides and sulfonamides as potential antitrypanosomal agents. J Med Chem 55(11):5554–5565. https://doi.org/10.1021/jm300508n

Patil S, Jadhav S, Patil P (2012) "Natural Acid Catalyzed Synthesis of Schiff Base under Solvent-freeCondition As a Green Approach" Arch. of Appl. Sci. Res. 4:1074–1078

Pal R, Khasnobis S, & Sarkar T (2013) "First Application of Fruit Juice of Citrus limon for Facile and GreenSynthesis of Bis- and Tris(indolyl)methanes in Water" Chemistry Journal 3:1–12

Rajasekaran R, Chen YP (2015) Potential therapeutic targets and the role of technology in developing novel antileishmanial drugs. Drug Discov Today 20(8):958–968. https://doi.org/10.1016/j.drudis.2015.04.006

Sachdeva H, Dwivedi D, Saroj R (2013a) Alum catalyzed simple, efficient, and green synthesis of 2-[3-amino-5-methyl-5-(pyridin-3-yl)-1,5-dihydro-4H-1,2,4-triazol-4-yl]propanoic acid derivatives in aqueous media. ScientificWorldJ 2013:716389. https://doi.org/10.1155/2013/716389

Sachdeva H, Saroj R, Khaturia S, Dwivedi D (2013b) Environ-economic synthesis and characterization of some new 1,2,4-triazole derivatives as organic fluorescent materials and potent fungicidal agents. Org Chem Int 2013:19. https://doi.org/10.1155/2013/659107

Salerno C, Carlucci A, Gorzalczany S, Bregni C (2014) In vitro inhibition of Leishmania braziliensis promastigotes growth by a fluconazole microemulsion. J Mol Pharm Org Process Res 2:115. https://doi.org/10.4172/2329-9053.1000115

Shams el-Dine SA, Hazzaa AA (1974) Synthesis of compounds with potential fungicidal activity. Part 2 Pharm 29(12):761–763

Shivarama Holla B, Veerendra B, Shivananda MK, Poojary B (2003) Synthesis characterization and anticancer activity studies on some Mannich bases derived from 1,2,4-triazoles. Eur J Med Chem 38 (7-8):759–767

Shokri A, Emami S, Fakhar M, Teshnizi SH, Keighobadi M (2017) In vitro antileishmanial activity of novel azoles (3-imidazolyl-flavanones) against promastigote and amastigote stages of Leishmania major. Acta Trop 167:73–78. https://doi.org/10.1016/j.actatropica.2016.12.027

Sun D-G, Hui X-P, Xu P-F, Zhang Z-Y, Guan Z-W (2007) Synthesis of novel biphenyltetrazole derivatives containing 5-methylisoxazole substituted 1,2,4-triazole. J Chin Chem Soc 54 (3):795–801. https://doi.org/10.1002/jccs.200700115

Szakacs G, Varadi A, Ozvegy-Laczka C, Sarkadi B (2008) The role of ABC transporters in drug absorption, distribution, metabolism, excretion and toxicity (ADME-Tox). Drug Discov Today 13(9-10):379–393. https://doi.org/10.1016/j.drudis.2007.12.010

Teague SJ, Davis AM, Leeson PD, Oprea T (1999) The design of leadlike combinatorial libraries. Angew Chem Int Ed Engl 38 (24):3743–3748

Testa B, Kraemer SD (2007) The biochemistry of drug metabolism—an introduction. Chemistry & Biodiversity Wiley Online Library 4: 2031-2122 https://doi.org/10.1002/cbdv.200790169

Veber DF, Johnson SR, Cheng HY, Smith BR, Ward KW, Kopple KD (2002) Molecular properties that influence the oral bioavailability of drug candidates. J Med Chem 45(12):2615–2623

Walker J, Gongora R, Vasquez JJ, Drummelsmith J, Burchmore R, Roy G, Ouellette M, Gomez MA, Saravia NG (2012) Discovery of factors linked to antimony resistance in Leishmania panamensis through differential proteome analysis. Mol Biochem Parasitol 183(2):166–176. https://doi.org/10.1016/j.molbiopara.2012.03.002

Wolf CR, Smith G, Smith RL (2000) Pharmacogenetics. Br Med J